Research Article | Vol. 30, No. 16 / 1 Aug 2022 / Optics Express 28710
Optics EXPRESS

Simultaneous measurement of torsion and strain at high temperature by using a highly birefringent cladding fiber Bragg grating

BAIJIE XU,[1,2] JUN HE,[1,2,*] XIZHEN XU,[1,2] JIA HE,[1,2] KUIKUI GUO,[1,2] WEIJIA BAO,[1,3] RUNXIAO CHEN,[1,2] SHEN LIU,[1,2] CHANGRUI LIAO,[1,2] AND YIPING WANG[1,2]

[1]*Key Laboratory of Optoelectronic Devices and Systems of Ministry of Education/Guangdong Province, College of Physics and Optoelectronic Engineering, Shenzhen University, Shenzhen 518060, China*
[2]*Shenzhen Key Laboratory of Photonic Devices and Sensing Systems for Internet of Things, Guangdong and Hong Kong Joint Research Centre for Optical Fibre Sensors, Shenzhen University, Shenzhen 518060, China*
[3]*School of Physics, Northwest University, Xi'an, 710127, China*
[*]*hejun07@szu.edu.cn*

Abstract: We demonstrate the fabrication of a new highly birefringent cladding fiber Bragg grating (Hi-Bi CFBG) consisting of a pair of sawtooth stressors near the fiber core by using a femtosecond laser direct writing technology. The unique sawtooth structure serves as in-fiber stressor and also generates Bragg resonance due to its periodicity. After optimization of laser pulse energy, the Hi-Bi CFBG with a high birefringence of 2.2×10^{-4} and a low peak reflectivity of ~ -24.5 dB (corresponding to ~ 0.3%) was successfully fabricated in a conventional single-mode fiber (SMF). And then, a wavelength-division-multiplexed Hi-Bi CFBGs array and an identical Hi-Bi CFBGs array were successfully constructed. Moreover, a simultaneous measurement of torsion and strain at high temperature of 700 °C was realized by using the fabricated Hi-Bi CFBG, in which the torsion can be deduced by monitoring the reflection difference between the two polarization peaks and strain can be detected by measuring polarization peak wavelength. A high torsion sensitivity of up to 80.02 dB/(deg/mm) and a strain sensitivity of 1.06 pm/με were achieved. As such, the proposed Hi-Bi CFBG can be used as a mechanical sensor in many areas, especially in structural health monitoring at extreme conditions.

1. Introduction

Multi-parameter measurements such as torsion and strain at high-temperature are required in structural health monitoring for hypersonic aircraft and aerospace vehicles. The surface temperature of the hypersonic aircraft at speeds above Mach 6 will exceed 530 °C, and the turbine blade of an aerospace vehicles engine will exceed 700 °C [1,2]. How to achieve a structural health monitoring at this extreme condition remains a problem. Recently, fiber-optic mechanical sensors are attractive due to the unique advantages of high sensitivity, compact size and immunity to electromagnetic interference [3]. For example, in-fiber Mach–Zehnder interferometers (MZIs) with microstructures, such as tapers and off-axis twist, are developed for simultaneous measurement of torsion and strain [4,5]. However, these MZIs with processed optical fibers have low mechanical strength, which is not conducive to practical application. Meanwhile, long-period fiber gratings (LPGs)-based in-fiber mechanical sensors have also been proposed, such as using a long LPG, a helical LPG or cascaded helical LPGs [6–8]. However, these sensors are sensitive to the external environment and usually suffer from the cross sensitivity to temperature. In recent years, mechanical sensors based on highly birefringent fiber Bragg gratings (Hi-Bi FBGs) have received considerable attention due to its robust structure and temperature insensitivity [9–14]. The torsion angle and direction can be determined simultaneously by

#464866 https://doi.org/10.1364/OE.464866
Journal © 2022 Received 25 May 2022; revised 1 Jul 2022; accepted 5 Jul 2022; published 20 Jul 2022

Optics EXPRESS

detecting the evolution of polarization dependent loss [11,12], reflectivity [13] or transmissivity [14] of Hi-Bi FBG. Note that temperature only causes the wavelength shift of Hi-Bi FBGs. However, these UV-induced Hi-Bi FBGs cannot withstand a high temperature above 450 °C [15].

Femtosecond laser, featuring by ultra-short pulse width and extremely high peak intensity, is a powerful tool for fabricating various microstructures based on optical fibers, including FBG, F-P interferometer and waveguide [16–18]. Note that femtosecond laser-inscribed Hi-Bi FBGs can operate at high temperatures [16]. Moreover, femtosecond laser direct writing technology is a more flexible method to fabricate Hi-Bi FBG [19–21]. For example, Chah *et al.* [21] reported a Hi-Bi FBG with a birefringence of 7.93×10^{-4} fabricated by using a femtosecond laser line-by-line technique. Nevertheless, it should be noted that these Hi-Bi FBGs fabricated in the fiber core always have a high reflectivity, which is detrimental to large-scale multiplexing. The ultra-weak FBGs, including high-order FBG and cladding FBG, were proposed to overcome this drawback [22–24]. For example, Chen *et al.* [24] demonstrated a cladding FBG with a peak reflectivity lower than -40 dB, but it only exhibited a low birefringence of 10^{-5}. However, the birefringence can be improved by inscribing stress lods, stress lines and sawtooth stressors in the fiber cladding by using a femtosecond laser direct writing technology [25–27]. Nevertheless, the fabrication process of this device is relatively complex since it includes two steps, i.e., fabricating FBG in fiber core and inscribing stressors in fiber cladding. In addition, these Hi-Bi FBGs also exhibited high reflectivity.

In this Letter, we propose and demonstrate a new method for fabricating a highly birefringent cladding fiber Bragg grating (Hi-Bi CFBG) with low reflectivity by using a femtosecond laser direct writing technology. After optimization of laser pulse energy, the Hi-Bi CFBG, consisting of a pair of sawtooth stressors near the fiber core, was successfully fabricated, and exhibited a high birefringence of 2.2×10^{-4} and a low reflectivity of ~ -24.5 dB (corresponding to ~ 0.3%). And then, a wavelength-division-multiplexed (WDM) Hi-Bi CFBGs array and an identical Hi-Bi CFBGs array were successfully constructed. Moreover, the Hi-Bi CFBG was used for simultaneous measurement of torsion and strain at high temperature of 700 °C and it exhibited a high torsion sensitivity of up to 80.02 dB/(deg/mm) and a strain sensitivity of 1.06 pm/με at high temperature of 700 °C.

2. Experimental setup for fabricating Hi-Bi CFBGs

Figure 1 shows the experimental setup for Hi-Bi CFBGs inscription with a femtosecond laser direct writing technology. In this setup, a frequency-doubled regenerative amplified Yb:KGW ($KGd(WO_3)$) femtosecond laser (Pharos, Light-conversion) with a wavelength of 514 nm, a pulse width of 290 fs, and a repetition rate of 200 kHz was employed. A 100× Leica oil-immersion objective with a numerical aperture (N.A.) of 1.25 was used as the focusing element. In addition, reflective index oil (n≈1.4587) is used to eliminate aberration induce by the cylindrical geometry of an optical fiber. The optical fiber is clamped by a pair of fiber holders mounted on a three-dimensional air-bearing translation stage (assembled by Aerotech ABL15010, ANT130LZS, and ANT130V-5). Moreover, a commercial OFDR (LUNA, OBR4600) was used to interrogate Hi-Bi CFBGs. The process for fabricating a Hi-Bi CFBG in the SMF is also illustrated in Fig. 1. The femtosecond laser beam was focused into the fiber cladding and the SMF was translated in a sawtooth trajectory via synchronous movements along the x-axis and y-axis. And then, a sawtooth structure, with a track length of L, a track tilted angle of θ and a pitch of Λ, was created in the cladding on one side of fiber core. Moreover, the same sawtooth structure was created in another side cladding. Such a pair of sawtooth structures can introduce an additional birefringence in the fiber core and provide a periodic refractive index modulation. As shown in the inset (a) of Fig. 1, a pair of sawtooth structures provide a periodic structure with a track length of 10.7 μm, a track tilted angle of 30° and a pitch of 10.7 μm, which can yield a Hi-Bi Bragg grating resonance. Moreover, we measured the refractive index distribution in the fabricated

Optics EXPRESS

Hi-Bi CFBG by using digital holographic microscopy (SHR-1602, index accuracy: 10^{-4}). In this equipment, the optimal digital hologram was obtained from the phase projection distribution of the test fiber, and the refractive index distribution in the fiber was calculated by using an angular spectrum theory-based algorithm and a filtered backprojection algorithm [28]. As shown in the inset (b) of Fig. 1, a step-index profile with positive and negative refractive index changes could be observed in the cross-sectional refractive index distribution. It could be seen that a pair of stressors can increase the refractive index in the sawtooth plane (i.e., slow axis) due to the stress-induced effects [29], which is higher than the refractive index in the plane orthogonal to the sawtooth stressors (i.e., fast axis).

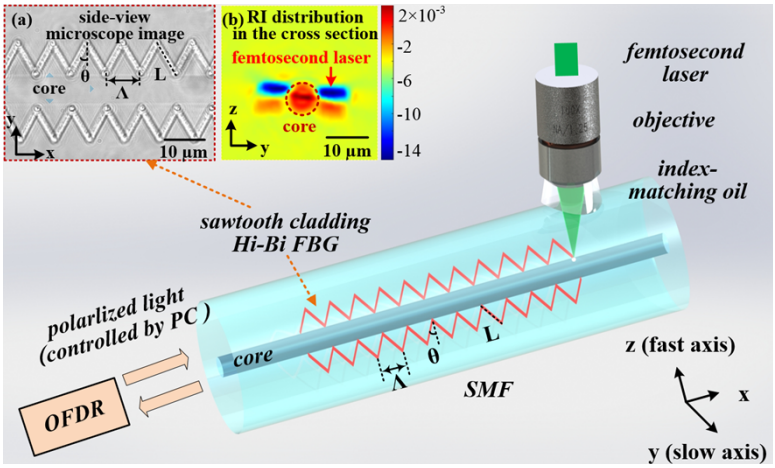

Fig. 1. Schematic of a Hi-Bi CFBG created in the conventional SMF by using a femtosecond laser direct writing technology. (Insets: (a) side-view microscope image of a sample fabricated by using a pulse energy of 44.0 nJ; (b) refractive index distribution in the cross section.)

3. Device fabrication and characterization

At first, four Hi-Bi CFBGs S1-S4 with the same track length of 10.7 μm, a track tilted angle of 30°, a pitch of 10.7 μm and total length of 5 mm were fabricated by using the increasing pulse energies E of 25.6, 34.9, 44.0 and 57.0 nJ, respectively. As shown in Figs. 2(a1)-2(a4), these tracks in Hi-Bi CFBGs S1-S4 are symmetric and closed to the fiber core. Note that the grating order of the fabricated Hi-Bi CFBG is 20. The reflection spectra of Hi-Bi CFBGs S1-S4 were measured by using OFDR and shown in Figs. 2(b1)-2(b4), respectively. In the case of Hi-Bi CFBG S1 fabricated by using a lower pulse energy, as shown in Fig. 2(b1), a polarization splitting of the reflection peak is not obvious, which indicates that a relatively low birefringence could be induced in S1. When the pulse energy increased to 34.9 nJ, as shown in Fig. 2(b2), the reflection peak of S2 exhibits an observable polarization splitting of the reflection peak $\Delta\lambda$ of 178 pm, which corresponds to a birefringence B of 1.7×10^{-4}. Moreover, in the case of Hi-Bi CFBGs S3 and S4 fabricated by higher pulse energy E of 44.0 and 57.0 nJ, these two samples show polarization splitting of the reflection peak $\Delta\lambda$ of 233 pm and 299 pm, respectively. It means that their birefringence of S3 and S4 are up to 2.2×10^{-4} and 2.8×10^{-4}, respectively, which is close to that in a commercial polarization maintaining fiber (i.e., $B = 3.2 \times 10^{-4}$) [30]. However, FBGs fabricated by using higher pulse energy have larger insertion loss. Hence, we chose Hi-Bi CFBG S3 for subsequent experiments.

Optics EXPRESS

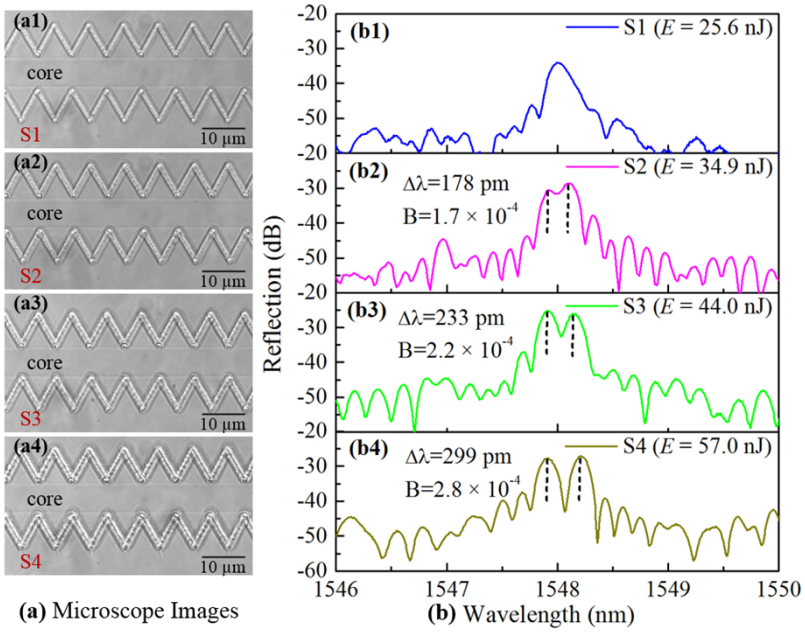

Fig. 2. Microscope images and reflection spectra of Hi-Bi CFBGs S1-S4 fabricated by using increasing pulse energies of 25.6, 34.9, 44.0 and 57.0 nJ, respectively: (a) side-view microscope images and (b) corresponding reflection spectra of S1-S4.

Subsequently, we characterized the reflection spectra of the fabricated Hi-Bi CFBG S3 by using an OFDR interrogator and a polarization controller (PC). In this experiment, when the input light with polarization along the fast axis was launched into S3, only one reflection peak with Bragg wavelength of 1547.708 nm can be observed, as shown in blue dotted line in Fig. 3(a). And then, the polarization of input light was adjusted to the slow axis and only one reflection peak with Bragg wavelength of 1547.941 nm can be observed, as shown in green dotted line in Fig. 3(a). Note that similar peak reflectivity of ~ -21.7 dB can be observed in the two curves. In addition, as displayed in red line in Fig. 3(a), in the case of the input light with 45° linear polarization, the two peaks with similar reflectivity of -24.5 dB are separated by 233 pm, yielding a birefringence value equal to 2.2×10^{-4}. Therefore, the spectra of Hi-Bi CFBG are strongly dependent on the polarization state of the input light.

Furthermore, we fabricated a WDM Hi-Bi CFBG array and an identical Hi-Bi CFBG array in SMF. The reflection spectra of these two arrays were measured by using OFDR. This WDM Hi-Bi CFBG array includes four 5 mm long Hi-Bi CFBGs (i.e., S5, S6, S7, and S8) with a spacing of 10 mm between the adjacent Bragg gratings and varying grating pitches Λ of 10.66, 10.68, 10.70 and 10.72 μm, respectively. As shown in Fig. 3(b), the Bragg wavelengths of polarization peak at fast axis of S5, S6, S7, and S8 were measured as 1542.0, 1544.9, 1547.8 and 1550.6 nm respectively. Moreover, an identical Hi-Bi CFBG array consisting of five Hi-Bi CFBGs (i.e., S9, S10, S11, S12 and S13) with the same pitch of 10.70 μm was successfully fabricated in a SMF by using the same pulse energy of 44.0 nJ. The demodulation results of the identical Hi-Bi CFBG array in spatial domain are shown in Fig. 3(c), in which these Hi-Bi FBGs with a grating length of 5 mm and a spacing of 10 mm could be observed. Additionally, a low amplitude in the S13 could be observed. This may result from the accumulation of transmission loss of Hi-Bi FBGs before S13. Moreover, as shown in Fig. 3(d), the reflection spectra of each Hi-Bi CFBG could be reconstructed. All of them exhibit two polarization peaks with the same Bragg wavelengths

Optics EXPRESS

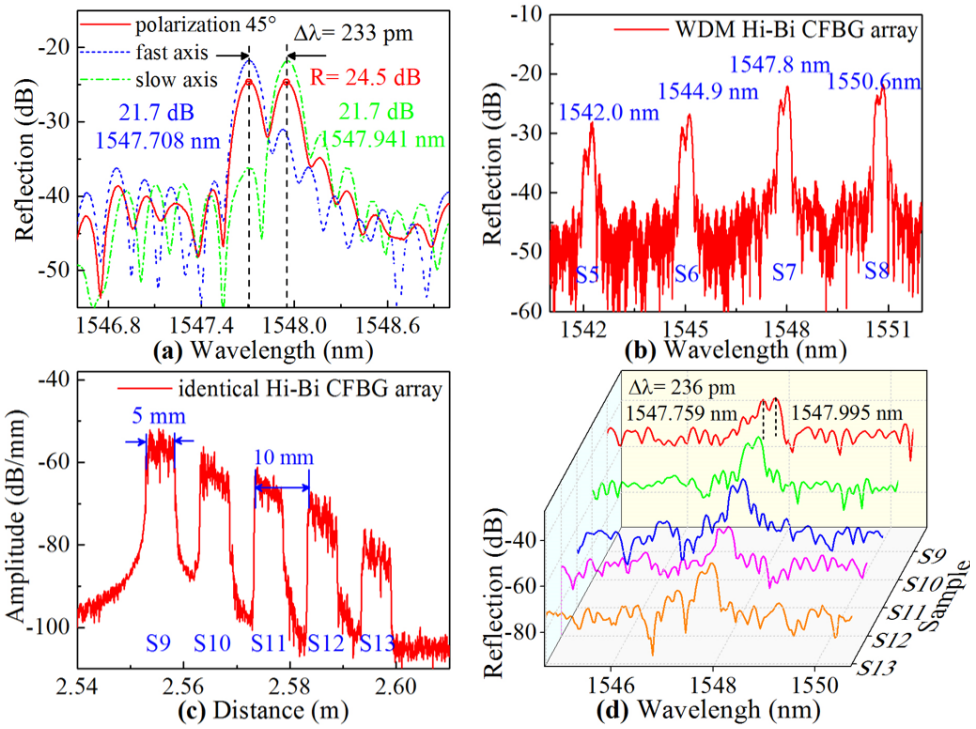

Fig. 3. Reflection spectra of (a) Hi-Bi S3 in three different polarizations and (b) the WDM Hi-Bi CFBG array. (c) Demodulation result of the identical Hi-Bi CFBG array in spatial domain. (d) Reflection spectra of each Hi-Bi CFBG in the identical Hi-Bi CFBG array.

of 1547.759 and 1547.995 nm, respectively. A few types of Hi-Bi FBGs were presented in Table 1. To the best of our knowledge, our current Hi-Bi CFBG exhibits the lowest reflectivity of 0.3%, which owes that our proposed sawtooth stressors is created in cladding. Note that this is beneficial for multiplexing. Moreover, such a Hi-Bi CFBG exhibit a birefringence of 2.8×10^{-4}, which is similar with the FBG induced in polarization maintaining fiber (PMF).

Table 1. A few types of Hi-Bi FBGs

Fabrication Method	Fiber Type	Hi-Bi FBG	Birefringence	Reflectivity	Reference
UV laser phase-mask	PMF	FBG	$\sim 5.46 \times 10^{-4}$	86.5%	[10]
UV laser phase-mask and femtosecond laser direct writing	SMF	FBG + stressor	2.96×10^{-4}	~90.0%	[27]
Femtosecond laser phase mask	PCF	FBG	1.05×10^{-3}	~68.0%	[20]
Femtosecond laser direct writing	SMF	FBG + stressor	2×10^{-3}	-	[26]
Femtosecond laser LbL method	SMF	FBG	7.93×10^{-4}	~29.2%	[21]
Femtosecond laser direct writing	**SMF**	**Sawtooth stressors**	$\mathbf{2.8 \times 10^{-4}}$	**~0.3%**	**This work**

4. Simultaneous measurement of torsion and strain at high temperature

We established an experimental setup for investigating the torsion and strain responses of the fabricated Hi-Bi CFBG S3 at high temperature of 700 °C. Note that the silica fiber would be

Optics EXPRESS

elongated under strain at a high temperature of up to 700 °C due to the viscous relaxation of silica [31]. Hence, the simultaneous measurement of torsion and strain was carried out at 700 °C. As shown in Fig. 4, the device under test (DUT) was placed in the center of tube furnace (Carbolite 301) by threading the fiber through an alundum tube and the temperature was maintained at 700 °C. In addition, the DUT was clamped by a pair of fiber rotators mounted on a one-dimensional translation stage for achieving simultaneous measurement of torsion and strain. The spectra evolutions were investigated by using OFDR and a PC when the DUT was under various torsion and strain. Note that the original polarization state of the input light should be carefully adjusted by using the PC to ensure both of the two polarization peaks achieve similar reflection amplitude at the same time.

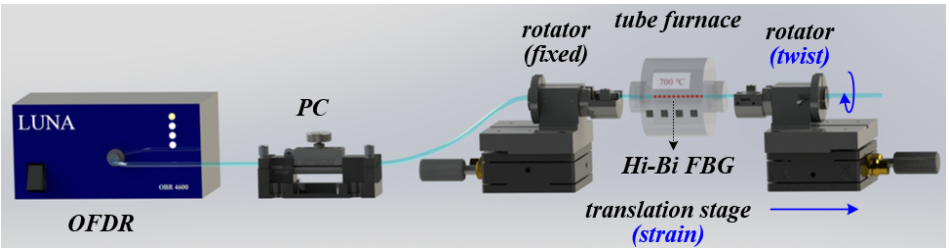

Fig. 4. Experimental setup for testing the torsion and strain response at high temperature of the fabricated Hi-Bi CFBG S3.

Subsequently, we investigated the torsion responses of the fabricated Hi-Bi CFBG S3 at high temperature of 700 °C. The S3 was twisted with an angle ranging from -180° to 180° in steps of 15°. Note that the two polarization peaks labeled as R1 and R2 exhibit an opposite evolution, as shown in Fig. 5(a), which can be used for recognition of the twist direction (i.e., clockwise and anticlockwise). The complete torsion response of the S3 from -180° to 180° is demonstrated in Fig. 5(b). It can be clearly seen that the reflection difference (i.e., R1-R2) changes with the torsion angle as a sine-like function. Here, the fabricated Hi-Bi CFBG acts as a polarization analyzer and the torsion would cause the rotation of principal axis of Hi-Bi CFBG relative to the orientation of input linear polarization state. Hence, the reflection difference of the two polarization peaks exhibits a sinusoidal relationship with torsion angle [13,19]. In addition, given that the twisted fiber length of 530 mm, the reflection difference could be regarded as a linear function of the torsion angle with a slope of 80.02 dB/(deg/mm) ranging from -90° to 90°, as shown in Fig. 5(c). In the process of torsion sensing, as shown in Fig. 5(d), the variation of Bragg wavelengths of two polarization peaks are less than 26 pm, which may be caused by the temperature fluctuation in furnace.

Additionally, we investigated the strain sensing characteristics of the Hi-Bi CFBG S3 at high temperature of 700 °C. The strain responses were tested by stretching the fiber, ranging from 0 to 775 με in steps of 75 με. As shown in Fig. 6(a), the reflection spectra of the S3 exhibit a 'red' shift with an increasing strain from 75 to 775 με. The measured results are well fitted by linear curves, and the Bragg wavelengths of two reflection peaks show the same strain sensitivity of 1.06 pm/με, as shown in Fig. 6(b). Moreover, the reflection amplitude of two polarization peaks is almost unchanged (i.e., < 0.44 dB) in the process of strain sensing, as displayed in Fig. 6(c).

A demodulation matrix can be established based on the obtained sensitivity coefficients:

$$\begin{bmatrix} \Delta T \\ \Delta S \end{bmatrix} = \begin{bmatrix} 80.02\text{dB/(deg/mm)} & 0 \\ 0 & 1.06\text{pm}/\mu\varepsilon \end{bmatrix}^{-1} \begin{bmatrix} \Delta R \\ \Delta \lambda \end{bmatrix}, \quad (1)$$

Optics EXPRESS

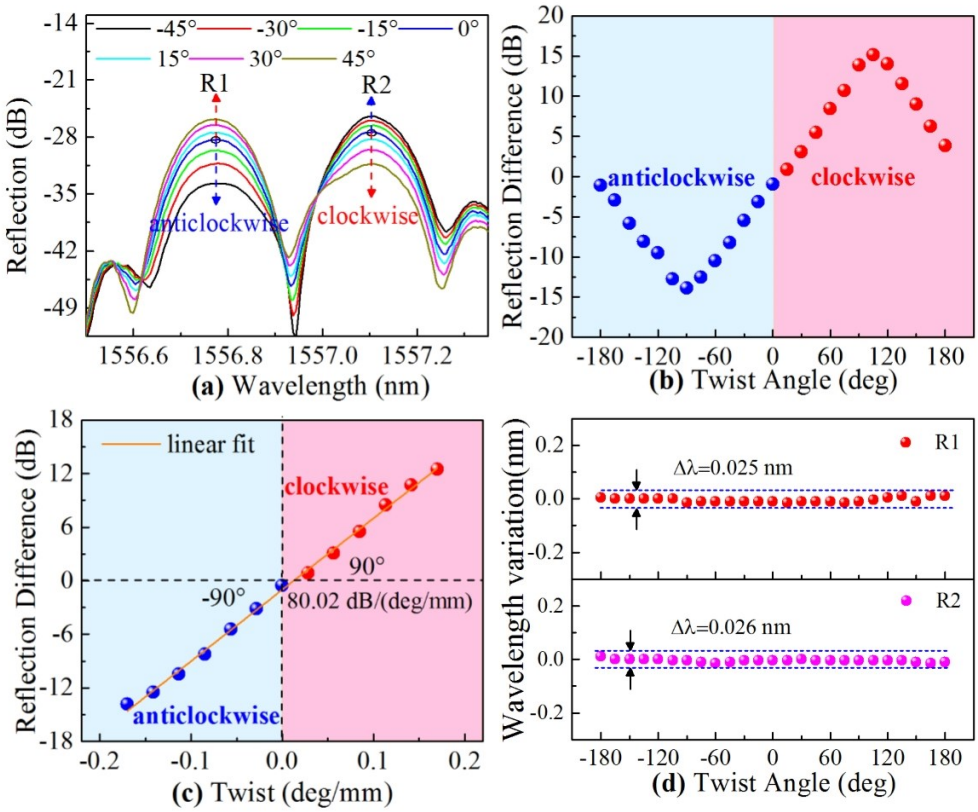

Fig. 5. Torsion sensing of the fabricated Hi-Bi CFBG S3 under applied torsion angle ranging from -180° to 180°at high temperature of 700 °C: the evolution of (a) reflection spectra and (b) reflection difference R1-R2; (c) the reflection difference R1-R2 as functions of torsion rate ranging from -0.196 to 0.196 deg/mm and (d) the fluctuations in Bragg wavelength of two polarization peaks.

where ΔT and ΔS represent the variation of torsion and strain, and ΔR and $\Delta\lambda$ are the corresponding reflection difference change and wavelength shift of two polarization peaks of the fabricated Hi-Bi CFBG, respectively. Hence, simultaneous measurement of torsion and strain could be achieved by using this demodulation matrix. Furthermore, the strain with a range of 75 to 675 με and the torsion angles with 0°, 30°, 60° and 90° were applied to the S3 simultaneously. It can be seen from Fig. 7(a) that the reflection difference increases with increasing torsion angle. Here, it only exhibits a slight change at various strains, resulting from the instability in the polarization state of the input light. Moreover, as shown in Fig. 7(b), the Bragg wavelength of one polarization peak R1 exhibits red shifts with the increasing strains, and remains stable at the various torsion angles. Therefore, these results demonstrate that the proposed Hi-Bi CFBG can be employed for simultaneous measurement of torsion and strain at high temperature of 700 °C.

Optics EXPRESS

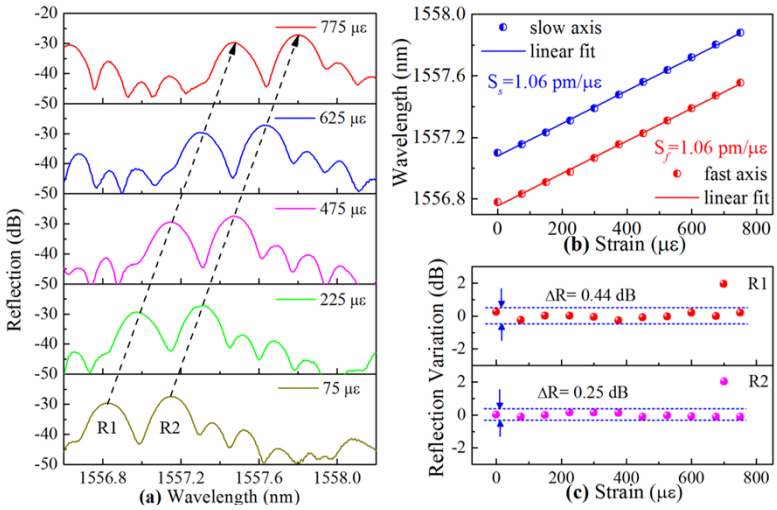

Fig. 6. Strain sensing of the fabricated Hi-Bi CFBG S3 under applied strain ranging from 0 to775 με at high temperature of 700 °C: (a) the evolutions of reflection spectra, (b) the Bragg wavelength shift as functions of strain and (c) the fluctuations in reflections of two polarization peaks.

5. Conclusion

We have successfully fabricated a new Hi-Bi CFBG consisting of a pair of sawtooth stressors near the fiber core in conventional SMF by using a femtosecond laser direct writing technology. Such a Hi-Bi CFBG exhibits a high birefringence of 2.2×10^{-4}, a significant polarization splitting of the reflection peak of 233 pm and a low reflectivity of -24.5 dB (corresponding to ~ 0.3%). And then, a WDM Hi-Bi CFBGs array and an identical Hi-Bi CFBG array were successfully constructed. Moreover, torsion and strain sensing characteristics of this device were studied at high temperature of 700 °C, and the results show that a high torsion sensitivity of up to 80.02 dB/(deg/mm) and a strain sensitivity of 1.06 pm/με could be achieved. As such, the proposed Hi-Bi CFBG can be used for simultaneous measurement of torsion and strain, which is promising for applying in many areas, especially in structural health monitoring at extreme environments.

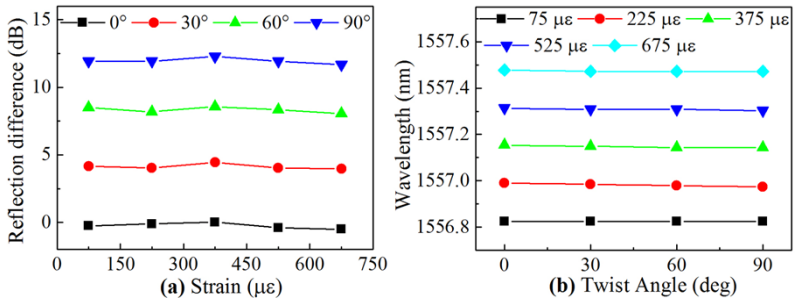

Fig. 7. Simultaneous measurement of torsion and strain at high temperature of 700 °C based on the fabricated Hi-Bi CFBG S3: the evolutions of (a) reflection difference R1-R2 and (b) Bragg wavelength R1 under different torsion angle ranging from 0° to 90° and strain ranging from 75 to 675 με.

Funding. National Natural Science Foundation of China (U191321261875128, 61905160); Guangdong Science and

Optics EXPRESS

Technology Department (2019TQ05X113, 2019A1515011393, 2019B1515120042,); Shenzhen Science and Technology Program (RCYX20200714114538160, JCYJ20210324120403009, JCYJ20210324100008024).

Disclosures. The authors declare no conflicts of interest.

Data availability. Data underlying the results presented in this paper are not publicly available at this time but maybe obtained from the authors upon reasonable request.

References

1. M. E. White and W. R. Price, "Affordable hypersonic missiles for long-range precision strike," Johns Hopkins APL Tech. Dig. **20**(3), 415–423 (1999).
2. N. Ejaz, I. N. Qureshi, and S. A. Rizvi, "Creep failure of low pressure turbine blade of an aircraft engine," Eng. Failure Anal. **18**(6), 1407–1414 (2011).
3. V. Budinski and D. Donlagic, "Fiber-optic sensors for measurements of torsion, twist and rotation: a review," Sensors **17**(3), 443 (2017).
4. Y. Liu, H. C. Deng, and L. B. Yuan, "Directional torsion and strain discrimination based on Mach-Zehnder interferometer with off-axis twisted deformations," Opt. Laser Technol. **120**, 105754 (2019).
5. P. Ghasemi and S. S. H. Yam, "Tension and torsion sensing with a double-taper Mach-Zehnder interferometer," J. Lightwave Technol. **40**(4), 1224–1230 (2022).
6. Y. P. Wang and Y. J. Rao, "Long period fibre grating torsion sensor measuring twist rate and determining twist direction simultaneously," Electron. Lett. **40**(3), 164–166 (2004).
7. Y. Y. Zhao, S. Liu, J. X. Luo, Y. P. Chen, C. L. Fu, C. Xiong, Y. P. Wang, S. Y. Jing, Z. Y. Bai, C. R. Liao, and Y. P. Wang, "Torsion, refractive index, and temperature sensors based on an improved helical long period fiber grating," J. Lightwave Technol. **38**(8), 2504–2510 (2020).
8. L. L. Xian, D. D. Wang, and L. Li, "Torsion and strain simultaneous measurement using a cascaded helical long-period grating," J. Opt. Soc. Am. B **37**(5), 1307–1311 (2020).
9. C. Caucheteur, T. Guo, and J. Albert, "Polarization-assisted fiber Bragg grating sensors: tutorial and review," J. Lightwave Technol. **35**(16), 3311–3322 (2017).
10. F. Yang, Z. J. Fang, Z. Q. Pan, Q. Ye, H. W. Cai, and R. H. Qu, "Orthogonal polarization mode coupling for pure twisted polarization maintaining fiber Bragg gratings," Opt. Express **20**(27), 28839–28845 (2012).
11. Y. P. Wang, X. Q. Huang, and M. Wang, "Temperature- and strain-independent torsion sensor utilising polarization-dependent," Electron. Lett. **49**(13), 840–841 (2013).
12. Y. P. Wang, M. Wang, and X. Q. Huang, "In fiber Bragg grating twist sensor based on analysis of polarization dependent loss," Opt. Express **21**(10), 11913–11920 (2013).
13. T. Guo, F. Liu, F. Du, Z. C. Zhang, C. J. Li, B. O. Guan, and J. Albert, "VCSEL-powered and polarization-maintaining fiber-optic grating vector rotation sensor," Opt. Express **21**(16), 19097–190102 (2013).
14. B. Yin, H. S. Li, S. C. Feng, Y. L. Bai, Z. B. Liu, W. J. Peng, S. Liu, and S. S. Jian, "Temperature-independent and strain-independent twist sensor based on structured PM-CFBG," IEEE Photonics Technol. Lett. **26**(15), 1565–1568 (2014).
15. J. Canning, "Fibre gratings and devices for sensors and lasers," Laser & Photon. Rev. **2**(4), 275–289 (2008).
16. C. Hnatovsky, D. Grobnic, and S. J. Mihailov, "Birefringent π-phase-shifted fiber Bragg gratings for sensing at 1000 °C fabricated using an infrared femtosecond laser and a phase mask," J. Lightwave Technol. **36**(23), 5697–5703 (2018).
17. C. R. Liao, C. Xiong, J. L. Zhao, M. Q. Zou, Y. Y. Zhao, B. Z. Li, P. Ji, Z. H. Cai, Z. S. Gan, Y. Wang, and Y. P. Wang, "Design and realization of 3D printed fiber-tip microcantilever probes applied to hydrogen sensing," Light: Adv. Manufac. **3**(1), 1 (2022).
18. O. Caulier, D. L. Coq, E. Bychkov, and P. Masselin, "Direct laser writing of buried waveguide in As_2S3 glass using a helical sample translation," Opt. Lett. **38**(20), 4212–4215 (2013).
19. B. Huang and X. W. Shu, "Ultra-compact strain- and temperature-insensitive torsion sensor based on a line-by-line inscribed phase-shifted FBG," Opt. Express **24**(16), 17670–17679 (2016).
20. D. Grobnic, H. Ding, S. J. Mihailov, C. W. Smelser, and J. Broeng, "High birefringence fibre Bragg gratings written in tapered photonic crystal fibre with femtosecond IR radiation," Electron. Lett. **43**(1), 16–17 (2007).
21. K. Chah, D. Kinet, M. Wuilpart, P. Megret, and C. Caucheteur, "Femtosecond-laser-induced highly birefringent Bragg gratings in standard optical fiber," Opt. Lett. **38**(4), 594–596 (2013).
22. B. J. Xu, J. He, B. Du, X. Z. Xiao, X. Z. Xu, C. L. Fu, J. He, C. R. Liao, and Y. P. Wang, "Femtosecond laser point-by-point inscription of an ultra-weak fiber Bragg grating array for distributed high-temperature sensing," Opt. Express **29**(20), 32615–32626 (2021).
23. F. Y. Chen, X. Y. Li, R. H. Wang, and X. G. Qiao, "Two-dimensional vector accelerometer based on orthogonal Bragg gratings inscribed in a standard single-mode fiber cladding," Opt. Lett. **46**(12), 2992–2995 (2021).
24. F. Y. Chen, X. Y. Li, R. H. Wang, and X. G. Qiao, "Multiple cladding fiber Bragg gratings inscribed by femtosecond laser point-by-point technology," J. Lightwave Technol. **39**(23), 1 (2021).
25. L. Yuan, B. K. Cheng, J. Huang, J. Liu, H. Z. Wang, X. W. Lan, and H. Xiao, "Stress-induced birefringence and fabrication of in-fiber polarization devices by controlled femtosecond laser irradiations," Opt. Express **24**(2), 1062–1071 (2016).

Optics EXPRESS

26. L. A. Fernandes, J. R. Grenier, P. V. S. Marques, J. S. Aitchison, and P. R. Herman, "Strong birefringence tuning of optical waveguides with femtosecond laser irradiation of bulk fused silica and single mode fibers," J. Lightwave Technol. **31**(22), 3563–3569 (2013).
27. K. K. Guo, J. He, L. P. Shao, G. X. Xu, and Y. P. Wang, "Simultaneous measurement of strain and temperature by a sawtooth stressor-assisted highly birefringent fiber Bragg grating," J. Lightwave Technol. **38**(7), 2060–2066 (2020).
28. C. Yan, S.-J. Huang, Z. Miao, Z. Chang, J. Z. Zeng, and T. Y. Wang, "3D refractive index measurements of special optical fibers," Opt. Fiber Technol. **31**, 65–73 (2016).
29. F. Chen and J. R. V. D. Aldana, "Optical waveguides in crystalline dielectric materials produced by femtosecond-laser micromachining," Laser Photonics Rev. **8**(2), 251–275 (2014).
30. E. Chehura, C. Ye, S. E. Staines, S. W. James, and R. P. Tatam, "Characterization of the response of fibre Bragg gratings fabricated in stress and geometrically induced high birefringence fibres to temperature and transverse load," Smart Mater. Struct. **13**(4), 888–895 (2004).
31. Z. R. Cui, J. H. Gong, C. Wang, N. N. Che, Y. S. Zhao, Q. Chai, H. F. Qi, E. Lewis, J. Ren, J. Z. Zhang, J. Yang, L. B. Yuan, and G. D. Peng, "Observing the viscous relaxation process of silica optical fiber at ~1000 °C using regenerated fiber Bragg grating," Sensors **19**(10), 2293 (2019).